

# Nonlinear optomechanical systems with quasi-periodic and chaotic dynamics

A.P. Saiko<sup>a,\*</sup>, G.A. Rusetsky<sup>a</sup>, S.A. Markevich<sup>a</sup>, R. Fedaruk<sup>b</sup>

<sup>a</sup>Scientific-Practical Material Research Centre, Belarus National Academy of Sciences, 19 P.Brovka str., Minsk, 220072, Belarus

<sup>b</sup>Institute of Molecular Physics, Polish Academy of Sciences, 17 Smoluchowski str., Poznan, 60-179, Poland

---

## Abstract

Model optomechanical systems, in which the coupling between an optical field and a mechanical resonator is described by linear, quadratic, and cubic terms in mechanical displacements, are studied. It is shown that under conditions for adiabatic elimination of the cavity field, the dynamics of the mechanical resonator is determined by some effective, generally bistable, potential. The shape of this potential depends on the power of the optical driving field, detuning between the cavity and driving frequencies, the parameters of nonlinear optomechanical interactions and the decay rate of the cavity field. Examples of both periodic and chaotic behavior of the mechanical resonator are illustrated by determining the power spectrum of mechanical oscillations, constructing the corresponding phase portraits and Poincaré maps.

*Keywords:* Nonlinear optics, Optomechanical interactions, Open systems, Dynamics and chaos

---

## 1. Introduction

Optomechanical systems offer the possibility for control of light by mechanical motion and vice versa [1]. The coupling between light and mechanical resonator (oscillator) vibrations is usually achieved via light pressure. The interaction between optical and mechanical modes leads to the implementation of various effects such as optomechanically induced transparency [2, 3, 4, 5, 6, 7, 8, 9], phonon lasers [10, 11, 12], normal-mode splitting [13, 14], photon blockade [15, 16, 17, 18, 19], mechanical resonator cooling [21, 22, 23], nonclassical state preparation [24, 25, 26, 27], and dynamic stabilization of a “membrane-in-the-middle” mechanical oscillator in an optical cavity [28]. Introducing the two-laser driving, controllable enhancement of the single-photon optomechanical coupling in a prototypical Fabry-Perot cavity was realized [29]. Optomechanical systems have potential applications in quantum information processing [30]. Collapses and revivals of mechanical motion and optical field in the optomechanical system have been described [31, 32].

A number of papers have been devoted to taking into account nonlinearities (cubic or fourth degree) of mechanical oscillators in optomechanical systems [33, 34], including studies of such effects as the generation of second-order sidebands [35], optomechanically induced transparency [36, 37], steady-state mechanical squeezing [38], optomechanical entanglement [39], formation of Kerr and cross-Kerr nonlinearities [40], and normal-mode splitting [41].

In recent years, a number of significant studies have been devoted to understanding the transition from classical nonlinear dynamics to chaotic dynamics in optomechanical systems (see,

for example, [42, 43]). The obtained results lay the foundation for the application of mechanical micro- and nanoresonators in sensing, for generating random numbers and data encryption based on optomechanics, optomechanical logic and chaos computing.

Most of optomechanical systems are based on the use of a parametric interaction, linear in mechanical displacement ( $\sim x$ ). In such systems, it is possible, for example, to cool the mechanical mode into its quantum ground state (with anti-Stokes pumping) or, conversely, to enhance the mechanical movement (with Stokes pumping). However, the optomechanical interaction is inherently nonlinear. Quantum nondemolition measurements are performed with quadratic interactions ( $\sim x^2$ ), which are usually implemented using membrane-in-the-middle configurations [6, 44]. Some fundamental problems may require optomechanical systems that involve higher order interactions, up to the third order in mechanical displacement ( $\sim x^3$ ) [45]. On the other hand, the intrinsic mechanical nonlinearity leads to the appearance of Kerr and cross-Kerr nonlinearities [40], as well as to collapses and revivals of the optical field in optomechanical systems [32].

Our aim is to study the dynamics of a mechanical oscillator in optomechanical systems, in which, in addition to the linear interaction, quadratic and cubic interactions of the oscillatory mode of the mechanical resonator with the mode of an optical cavity are taken into account. We focus on the unusual dynamics of the mechanical resonator when the type and magnitude of nonlinearity of the optomechanical interaction change. In particular, our studies show that the simultaneous presence of linear and quadratic optomechanical interactions leads to a chaotic regime of the dynamics of the mechanical resonator (at a fixed choice of the parameters of the optomechanical system and initial conditions). If, for example, due to symmetry restrictions, only the quadratic interaction is preserved, then the

---

\*Corresponding author.

Email address: saiko@physics.by (A.P. Saiko)

behavior of the mechanical resonator is intermediate between quasi-periodic and chaotic. It is interesting that the complex type of optomechanical interaction, when linear, quadratic and cubic couplings are taken into account simultaneously, does not lead to chaos in mechanical oscillations, but only to their multi-quasiperiodicity. Throughout we consider the situation where the cavity decay rate is much larger than the resonant frequency of the mechanical oscillator, and therefore adiabatic elimination of the cavity field is valid.

## 2. Theory

Let us consider a model optomechanical system in which, in addition to photon-phonon interactions, linear and quadratic in mechanical displacements, there is a noticeable "cubic interaction". Such optomechanical system consists of a mechanical oscillator with mass  $m$  and frequency  $\omega_m$  that is non-linearly coupled via optomechanical interactions to a single cavity mode. The Hamiltonian describing the system is [45]

$$\begin{aligned} H &= H_0 + V + V_{drive}^c, \quad (1) \\ H_0 &= \omega_c \hat{a}^\dagger \hat{a} + \frac{1}{2} \left( \frac{\hat{p}^2}{m} + m\omega_m^2 \hat{x}^2 \right), \\ V &= -\hat{a}^\dagger \hat{a} \left[ g_1 \hat{x} + \frac{g_2}{2} \hat{x}^2 + \frac{g_3}{6} \hat{x}^3 \right], \\ V_{drive}^c &= i\varepsilon (\hat{a}^\dagger e^{-i\omega_d t} - H.c.), \end{aligned}$$

where  $\omega_c$  is the cavity resonant frequency,  $g_i$  is the optomechanical coupling strength, linear ( $g_1$ ), quadratic ( $g_2$ ) and cubic ( $g_3$ ) in displacements of the mechanical oscillator, and  $a$  denotes the bosonic annihilation operator for the cavity field with  $[\hat{a}, \hat{a}^\dagger] = i$  (we take the Planck constant  $\hbar = 1$ ),  $\hat{x}$  and  $\hat{p}$  are the position and momentum operators for the mechanical oscillator with the commutation relation  $[\hat{x}, \hat{p}] = i$ . Here  $V_{drive}$  is the driving term where  $\varepsilon$  is the amplitude of the optical driving field.

The classical equations of motion are found by replacing operators by their c-number counterparts in the Heisenberg equations derived from the Hamiltonian (1), neglecting noise sources for now [28, 46]. In a frame rotating at the laser frequency  $\omega_d$ , the following classical equations for the position  $x$ , momentum  $p$ , and the intracavity field amplitude  $a$  can be written:

$$\frac{d}{dt}a = \left[ -i\Delta + i\varphi(x) - \frac{\kappa}{2} \right] a + \varepsilon, \quad (2)$$

$$\frac{d}{dt}x = \frac{p}{m}, \quad \frac{d}{dt}p = -m\omega_m^2 x + |a|^2 \psi(x) - \frac{\gamma}{2} p, \quad (3)$$

where

$$\varphi(x) = g_1 x + \frac{g_2}{2} x^2 + \frac{g_3}{6} x^3, \quad \psi(x) = \frac{d\varphi}{dx}, \quad (4)$$

$\Delta = \omega_c - \omega_d$  is the detuning between the cavity and laser frequencies,  $\kappa$  is the phenomenological decay rate of the cavity field, and  $\gamma$  is the mechanical damping rate.

If the cavity decay rate  $\kappa$  is much larger than the resonant frequency of the mechanical oscillator, the cavity field may be adiabatically eliminated on time scales longer than  $\kappa^{-1}$  to yield

$$\frac{d}{dt}p = -m\omega_m^2 x + \frac{2P\kappa/\omega_d}{[\Delta - \varphi(x)]^2 + \kappa^2/4} \psi(x) - \frac{\gamma}{2} p, \quad (5)$$

where  $P = \omega_d \varepsilon^2 / (2\kappa)$  is the continuous wave input power of the cavity. In the absence of mechanical dissipation,  $\gamma = 0$ , Eq. (5) can be written as  $dp/dt = -\partial U_{eff} / \partial x$ , where

$$U_{eff}(x) = \frac{m\omega_m^2}{2} x^2 + \frac{4P}{\omega_d} \arctan \left[ \frac{\Delta - \varphi(x)}{\kappa/2} \right]. \quad (6)$$

We see that the adiabatic elimination of the cavity field involves corresponding replacement of the initial mechanical potential  $m\omega_m^2 x^2 / 2$  by the effective mechanical potential  $U_{eff}(x)$  describing the dynamics of the mechanical mode. Thus, the effective potential is the sum of the harmonic potential and the term with arctangent function which can be controlled by the pump field, the detuning between the cavity and driving frequencies, the coupling constants  $g_i$ , and the cavity decay rate  $\kappa$ .

## 3. Results and discussion

Fig. 1 shows effects of the value and sign of the cubic optomechanical coupling strength  $g_3$  and the amplitude  $\varepsilon$  of the optical driving field on the shape of the effective mechanical potential  $U_{eff}(x)$ . To express all constants in energy (frequency) units, it is necessary to make the following substitution:  $g_i \rightarrow g_i (1/2m\omega_m)^{i/2}$ , where  $(1/2m\omega_m)^{1/2} \equiv x_{zpf}$  is the size of mechanical zero-point fluctuations. At the positive values of  $g_3$  (Fig. 1a), the effective potential has one minimum, and the mechanical oscillator has one stable state of equilibrium. With an increase in  $\varepsilon$ , the minimum shifts towards higher values of  $x$ . When the cubic coupling strength  $g_3$  becomes negative (Fig. 1c), the effective mechanical potential is transformed into a double-well one, and the mechanical oscillator can be in a metastable state. At  $g_3 = 0$  and  $g_1 = 0$  the potential has a symmetric two-minimum shape for arbitrary values of  $\varepsilon$ , but at  $g_1 \neq 0$ , an asymmetry appears in the location of the minima (Fig. 1b). This asymmetry increases with increasing the linear optomechanical coupling strength and the amplitude of the optical driving field. In all three cases shown in Fig. 1 ( $g_3$  is positive, zero and negative), in the absence of a driving field ( $\varepsilon = 0$ ) the potential is, of course, harmonic, i.e. equal to  $m\omega_m^2 x^2 / 2$ . Note that asymmetric double-well potentials similar to those discussed here are often encountered in condensed matter physics problems [47].

As in [28], we assume that the input power of the driving field is modulated with frequency  $\Omega$ , and  $\Omega \ll \kappa$ . Therefore, one can consider the non-stationary behavior of the mechanical resonator with a time-dependent potential if in Eq. (6) the input power parameter is represented as

$$P = \frac{\omega_d}{2\kappa} (\varepsilon^2 + \varepsilon_M^2 \sin \Omega t), \quad \varepsilon_M \leq \varepsilon, \quad (7)$$

where  $\varepsilon_M$  is the modulation field amplitude.

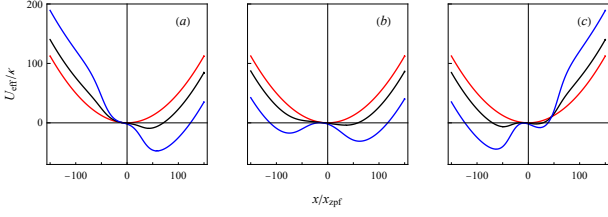


Figure 1: The effective mechanical potential at different cubic coupling strengths  $g_3$  and amplitudes  $\varepsilon/\kappa$  of the driving field. All parameters are normalized with respect to  $\omega_m \cdot \kappa = 50.0$ ,  $\omega_m = 1$ ,  $\Delta = -1.0$ ,  $g_1 = 0.15$  and  $g_2 = 0.015$ . Red, black and blue lines were obtained at  $\varepsilon/\kappa = 0, 3$  and  $5$ , respectively. (a)  $g_3 = 0.0015$ . (b)  $g_3 = 0$ . (c)  $g_3 = -0.0015$ .

When carrying out numerical calculations using Eqs. (5) – (7) to construct phase portraits, the time was maintained from 0 to 0.01 s. To construct Poincaré sections, strobing was carried out at moments of time  $t_n = (2\pi/\Omega)n$ , where integer values  $n$  varied from 1 to 1800 over 0.1 s.

The dynamics of the mechanical resonator in the optomechanical system when the Hamiltonian of the optomechanical interaction contains only the term that is linear in mechanical displacements is illustrated in Fig. 2. In this case, the effective potential of the mechanical resonator has a minimum that is somewhat shifted toward the positive region. The resonator oscillations are of a quasi-periodic nature. Their power spectrum contains a high-intensity main peak at the frequency  $\omega_m$  and a significantly weaker one at the driving field frequency  $\Omega$ , as well as a barely noticeable second harmonic of  $\omega_m$ . The Poincaré section has the shape of an almost ideal circle, shifted, like the phase portrait, into the positive region.

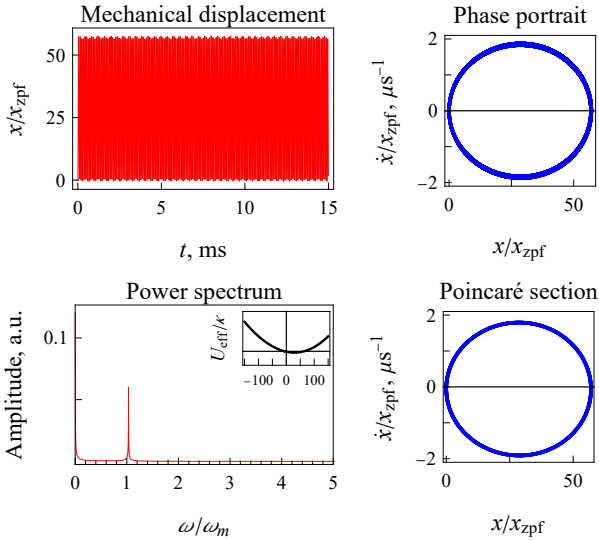


Figure 2: Dynamics of the mechanical oscillator when the optomechanical interaction contains only a linear term ( $g_1 = 0.15$ ,  $g_2 = g_3 = 0$ ). The inset shows the effective mechanical potential. All parameters are normalized with respect to  $\omega_m \cdot \kappa = 50.0$ ,  $\Delta = -1.0$ ,  $\varepsilon/\kappa = 5$ ,  $\varepsilon_M/\varepsilon = 0.20007$ , and  $\Omega = 1.8$ .

If the optomechanical interaction is quadratic in mechanical displacements, the corresponding anharmonic effective potential of the mechanical resonator has a symmetric double-well shape centered on  $x = 0$ . The shape of the power spectrum,

phase portrait and Poincaré section indicate the emerging transition from dynamic to chaotic behavior (Fig. 3). The time dependence of mechanical displacement shows that at first the mechanical resonator oscillates predominantly in the right well with infrequent transitions to the left well. Then, over time, the situation changes to the opposite, and a similar alternation of changes in the oscillatory positions of the mechanical system continues in the future. A structured continuous power spectrum is formed, and the phase portrait and Poincaré section take on the appearance of a slightly blurred figure eight, elongated along the  $x$  axis.

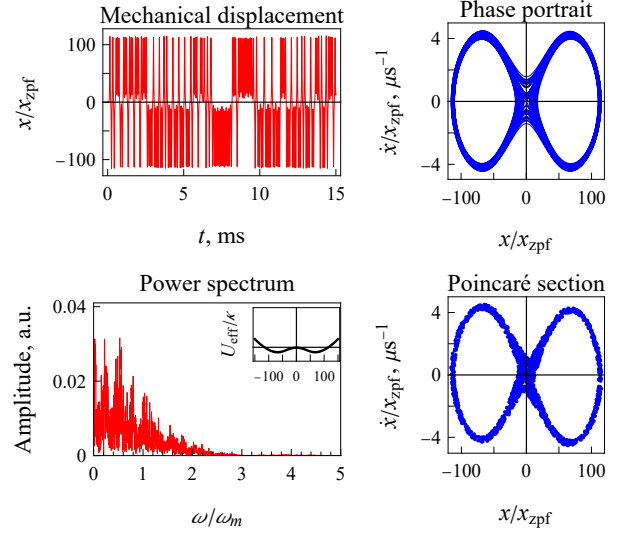


Figure 3: Dynamics of the mechanical oscillator when the optomechanical interaction contains only quadratic term ( $g_1 = g_3 = 0$ ,  $g_2 = 0.015$ ). The inset shows the effective mechanical potential. Other parameters are the same as in Fig. 2.

In the presence of only linear and quadratic terms in mechanical displacements in the optomechanical interaction, the symmetry of the double-well effective potential is broken: the right well drops slightly lower than the left one. The resonator oscillations remain chaotic in nature, and, compared to the previous case, the phase portrait and Poincaré section have the appearance of a slightly modified figure eight (Fig. 4). The time dependence of mechanical displacement indicates that, during the first ten milliseconds, the mechanical resonator performs quasi-harmonic oscillations in the right well. This is confirmed by the corresponding part of the power spectrum shown by the blue line. Next, there is an alternation of the presence of the chaotically oscillating mechanical resonator in the left or right wells with its somewhat predominant presence in the lower right well. The full power spectrum takes on a structured continuous shape.

If the optomechanical interaction contains linear, quadratic and cubic terms in mechanical displacements, the effective potential of the mechanical resonator for the selected set of system parameters has a global minimum and an inflection point on its relief (Fig. 5). In the power spectrum, in addition to the intense main peak at frequency  $\omega_m$  and the weaker one at frequency  $\Omega$ , there are their harmonics and subharmonics, and all

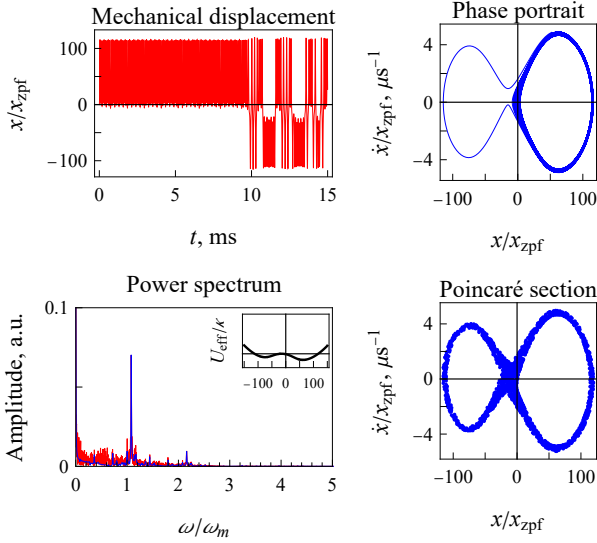


Figure 4: Dynamics of the mechanical oscillator when the optomechanical interaction contains linear and quadratic terms ( $g_1 = 0.15$ ,  $g_2 = 0.015$  and  $g_3 = 0$ ). The blue line in the power spectrum is the Fourier spectrum of mechanical displacement taken over the interval from 0 to 10 ms. The inset shows the effective mechanical potential. Other parameters are the same as in Fig. 2.

these peaks have their satellites on the left and right. The phase portrait consists of two fairly narrow closed bands inserted into each other in the positive region and connected near a point  $(\dot{x}, x) = (0, 0)$ . On the Poincaré plane, this phase portrait corresponds to three different lines, one of which is located near the point  $(\dot{x}, x) = (0, 0)$ , the second, longer one, is in the upper part of the Poincaré plane, and the third, the longest one, is in the lower part. Thus, a 3-quasiperiodic motion of the mechanical resonator is realized (Fig. 5).

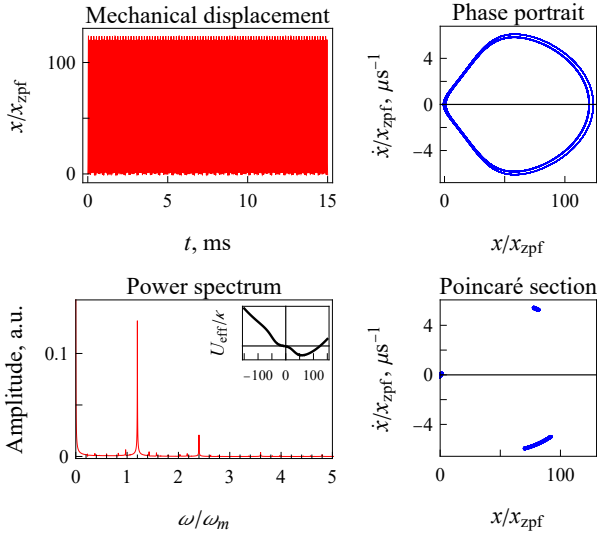


Figure 5: Dynamics of the mechanical oscillator.  $g_1 = 0.15$ ,  $g_2 = 0.015$  and  $g_3 = 0.0015$ . The inset shows the effective mechanical potential. Other parameters are the same as in Fig. 2.

It is interesting that the presence of all three types of the optomechanical interaction does not lead to chaoticization of the

oscillations of the mechanical resonator, as it happens in the presence of both linear and quadratic interactions (Fig. 4), or only quadratic interaction (Fig. 3).

The transition to chaotic oscillations of the mechanical resonator strongly depends on the amplitude of the modulating optical field. Fig. 6 shows phase portraits and Poincaré sections for the mechanical resonator when the amplitude of this field was increased by a factor of 2.5 compared to the case shown in Fig. 5. The results are given for the optomechanical system with  $g_3 > 0$  and  $g_3 < 0$ . At  $g_3 > 0$ , the minimum of the effective potential is shifted to the positive region of mechanical displacements (see Fig. 1a), and, accordingly, the phase portrait and the Poincaré section illustrate the chaotic motion of the mechanical resonator mainly in this region. When  $g_3 < 0$  and the two-minimum effective potential with the left global minimum is realized (see Fig. 1c), the phase portrait and the Poincaré section are mainly in the negative region of mechanical displacements, i.e. chaotic movements occur predominantly in the left global minimum.

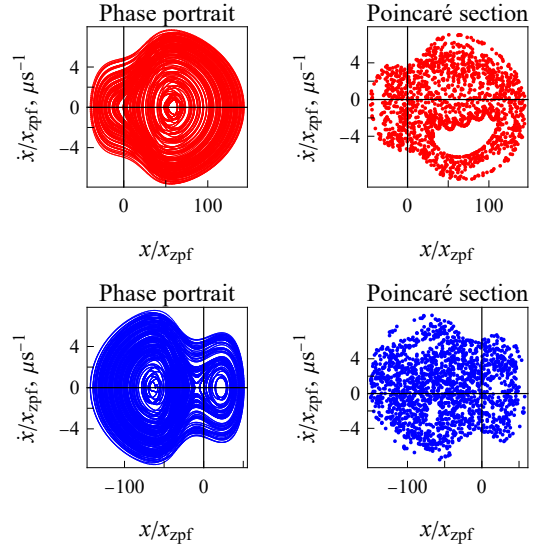


Figure 6: Phase portraits and Poincaré sections for the mechanical resonator at  $\varepsilon_M/\varepsilon = 0.5001$ ,  $g_1 = 0.15$ ,  $g_2 = 0.015$ ,  $g_3 = 0.0015$  (red plots) and  $g_3 = -0.0015$  (blue plots). Other parameters are the same as in Fig. 2.

## 4. Conclusion

We have studied model optomechanical systems with the photon-vibration interactions linear, quadratic, and cubic in mechanical displacements. It was found that under the conditions of adiabatic elimination of the cavity field, the dynamics of the mechanical resonator is determined by some effective potential. The transformation of this potential from single-well to double-well and bistable behavior of the mechanical oscillator were demonstrated. The transition of the mechanical resonator from dynamic to chaotic behavior was shown when “switching on” linear, quadratic and cubic (or their combination) optomechanical interactions in mechanical displacements with a certain choice of other parameters of the system under study and

initial conditions. Maintaining this set of parameters and initial conditions, we have found that the transition to the chaotic oscillation regime of the mechanical resonator is realized in the presence of both linear and quadratic interactions. In this case, the presence of only quadratic interaction is a boundary factor for the transition from dynamic to chaotic behavior. In any case, the transition to chaotic behavior is not realized without the presence of a quadratic term in mechanical displacements. The discovered features of nonlinear dynamics of optomechanical systems are important to the physics of open quantum systems as well as for possible practical applications, including sensors based on mechanical micro- and nanoresonators, optomechanical logic and chaos computing.

## References

- [1] M. Aspelmeyer, T.J. Kippenberg, F. Marquardt, Cavity optomechanics, *Eur. Phys. J. D* **86** (2014) 1391–1452.
- [2] S. Weis, R. Rivière, S. Deléglise, E. Gavartin, O. Arcizet, A. Schliesser, T.J. Kippenberg, Optomechanically induced transparency, *Science* **330** (2010) 1520–1523.
- [3] G.S. Agarwal, S. Huang, Electromagnetically induced transparency in mechanical effects of light, *Phys. Rev. A* **81** (2010) 041803(R).
- [4] A.H. Safavi-Naeini, T.P. Mayer Alegre, J. Chan, M. Eichenfield, M. Winger, Q. Lin, J.T. Hill, D.E. Chang, O. Painter, Electromagnetically induced transparency and slow light with optomechanics, *Nature* **472** (2011) 69–73.
- [5] A. Kronwald, F. Marquardt, Optomechanically induced transparency in the nonlinear quantum regime, *Phys. Rev. Lett.* **111** (2013) 133601.
- [6] M. Karuza, C. Biancofiore, M. Bawaj, C. Molinelli, M. Galassi, R. Natali, P. Tombesi, G. Di Giuseppe, D. Vitali, Optomechanically induced transparency in a membrane-in-the-middle setup at room temperature, *Phys. Rev. A* **88** (2013) 013804.
- [7] H. Jing, Ş.K. Özdemir, Z. Geng, J. Zhang, X.-Y. Lü, B. Peng, L. Yang, F. Nori, Optomechanically-induced transparency in parity-time-symmetric microresonators, *Sci. Rep.* **5** (2015) 9663.
- [8] H. Lü, C. Wang, L. Yang, H. Jing, Optomechanically Induced Transparency at Exceptional Points, *Phys. Rev. Appl.* **10** (2018) 014006.
- [9] C. Shang, H.Z. Shen, X.X. Yi, Nonreciprocity in a strongly coupled three-mode optomechanical circulatory system, *Opt. Express* **27**, (2019) 25882–25901.
- [10] C. Galland, N. Sangouard, N. Piro, N. Gisin, T.J. Kippenberg, Heralded single-phonon preparation, storage, readout in cavity optomechanics, *Phys. Rev. Lett.* **112** (2014) 143602.
- [11] H. Lü, S.K. Özdemir, L.-M. Kuang, F. Nori, H. Jing, Exceptional Points in Random-Defect Phonon Lasers, *Phys. Rev. Appl.* **8** (2017) 044020.
- [12] Y. Jiang, S. Maayani, T. Carmon, F. Nori, H. Jing, Nonreciprocal Phonon Laser, *Phys. Rev. Appl.* **10** (2018) 064037.
- [13] J.M. Dobrindt, I. Wilson-Rae, T.J. Kippenberg, Parametric normal-mode splitting in cavity optomechanics, *Phys. Rev. Lett.* **101** (2008) 263602.
- [14] S. Huang, G.S. Agarwal, Normal-mode splitting in a coupled system of a nanomechanical oscillator and a parametric amplifier cavity, *Phys. Rev. A* **80** (2009) 033807.
- [15] P. Rabl, Photon blockade effect in optomechanical systems, *Phys. Rev. Lett.* **107** (2011) 63601.
- [16] A. Nunnenkamp, K. Børkje, S.M. Girvin, Single-photon optomechanics, *Phys. Rev. Lett.* **107** (2011) 63602.
- [17] J.-Q. Liao, F. Nori, Photon blockade in quadratically coupled optomechanical systems, *Phys. Rev. A* **88** (2013) 023853.
- [18] D.-Y. Wang, C.-H. Bai, Y. Xing, S. Liu, S. Zhang, H.-F. Wang, Enhanced photon blockade via driving a trapped  $\Lambda$ -type atom in a hybrid optomechanical system, *Phys. Rev. A* **102** (2020) 043705.
- [19] H.Z. Shen, C. Shang, Y.H. Zhou, X.X. Yi, Unconventional single-photon blockade in non-Markovian systems, *Phys. Rev. A* **98** (2018) 23856.
- [20] A. Nunnenkamp, K. Børkje, S.M. Girvin, Cooling in the single-photon strong-coupling regime of cavity optomechanics, *Phys. Rev. A* **85** (2012) 051803.
- [21] Y.-C. Liu, Y.-F. Xiao, X. Luan, C.W. Wong, Dynamic Dissipative Cooling of a Mechanical Resonator in Strong Coupling Optomechanics, *Phys. Rev. Lett.* **110** (2013) 153606.
- [22] M.R. Vanner, J. Hofer, G.D. Cole, M. Aspelmeyer, Cooling-by-measurement and mechanical state tomography via pulsed optomechanics, *Nat. Commun.* **4**, 2295 (2013).
- [23] H.-K. Lau, A.A. Clerk, Ground-State Cooling and High-Fidelity Quantum Transduction via Parametrically Driven Bad-Cavity Optomechanics, *Phys. Rev. Lett.* **124** (2020) 103602.
- [24] J.-Q. Liao, L. Tian, Macroscopic Quantum Superposition in Cavity Optomechanics, *Phys. Rev. Lett.* **116** (2016) 163602.
- [25] M. Wang, X.-Y. Lü, Y.-D. Wang, J.Q. You, Y. Wu, Macroscopic quantum entanglement in modulated optomechanics, *Phys. Rev. A* **94** (2016) 053807.
- [26] I. Shomroni, L. Qiu, T.J. Kippenberg, Optomechanical generation of a mechanical catlike state by phonon subtraction, *Phys. Rev. A* **101** (2020) 033812.
- [27] J.T. Muhonen, G.R. La Gala, R. Leijssen, E. Verhagen, State Preparation and Tomography of a Nanomechanical Resonator with Fast Light Pulses, *Phys. Rev. Lett.* **123** (2019) 113601.
- [28] H. Seok, E.M. Wright, P. Meystre, Dynamic stabilization of an optomechanical oscillator, *Phys. Rev. A* **90** (2014) 043840.
- [29] C. Shang, Coupling enhancement and symmetrization of single-photon optomechanics in open quantum systems, *arXiv: 2302.04897* (2023) 1–19.
- [30] K. Stannigel, P. Komar, S.J.M. Habraken, S.D. Bennett, M.D. Lukin, P. Zoller, P. Rabl, Optomechanical quantum information processing with photons and phonons, *Phys. Rev. Lett.* **109** (2012) 13603.
- [31] J.D.P. Machado, R.J. Slioter, Y.M. Blanter, Quantum signatures in quadratic optomechanics, *Phys. Rev. A* **99** (2019) 053801.
- [32] A.P. Saiko, G.A. Rusetzky, S.A. Markevich, R. Fedaruk, Optomechanical systems with nonlinear interactions: photon blockade, collapse and revival of optical oscillations, *arXiv:2412.00908* (2024) 1–7.
- [33] L. Latmiral, F. Armata, M.G. Genoni, I. Pikovski, M.S. Kim, Probing anharmonicity of a quantum oscillator in an optomechanical cavity, *Phys. Rev. A* **93** (2016) 52306.
- [34] M. Grimm, C. Bruder, N. Lörch, Optomechanical self-oscillations in an anharmonic potential: engineering a nonclassical steady state, *New J. Phys.* **18** (2016) 94004.
- [35] Q. Zhao, Y. He, Y. Yang, H. Zhang, Y. Xu, Second-Order Sidebands and Group Delays in Coupled Optomechanical Cavity System with a Cubic Nonlinear Harmonic Oscillator, *Photonics* **11** (2024) 256.
- [36] S. Huang, H. Hao, A. Chen, The Optomechanical Response of a Cubic Anharmonic Oscillator, *Appl. Sci.* **10** (2020) 5719.
- [37] W. Lv, L. Deng, S. Huang, A. Chen, Optomechanically Induced Transparency in Optomechanical System with a Cubic Anharmonic Oscillator, *Photonics* **10** (2023) 407.
- [38] X.-Y. Lü, J.-Q. Liao, L. Tian, F. Nori, Steady-state mechanical squeezing in an optomechanical system via Duffing nonlinearity, *Phys. Rev. A* **91** 13834 (2015) 13834.
- [39] S. Huang, Y. Wu, A. Chen, The Stationary Optomechanical Entanglement Between an Optical Cavity Field and a Cubic Anharmonic Oscillator, *Int. J. Theor. Phys.* **60** 3961 (2021) 3961–3972.
- [40] A.P. Saiko, R. Fedaruk, S.A. Markevich, Kerr-Like Nonlinearities in an Optomechanical System with an Asymmetric Anharmonic Mechanical Resonator, *JETP Lett.* **113** (2021) 487–492.
- [41] H. Hao, S. Huang, A. Chen, Normal Mode Splitting in a Cavity Optomechanical System with a Cubic Anharmonic Oscillator, *Int. J. Theor. Phys.* **60** (2021) 2766–2777.
- [42] L. Bakemeier, A. Alvermann, H. Fehske, Route to chaos in optomechanics, *Phys. Rev. Lett.* **114** (2015) 13601.
- [43] G.-L. Zhu, C.-S. Hu, Y. Wu, X.-Y. Lü, Cavity optomechanical chaos, *Fundam. Res.* **3** (2023) 63–74.
- [44] M. Aspelmeyer, T.J. Kippenberg, F. Marquardt, Cavity optomechanics, *Rev. Mod. Phys.* **86** (2014) 1391.
- [45] D. Cattiaux, X. Zhou, S. Kumar, I. Golokolenov, R.R. Gazizulin, A. Luck, L.M. de Lépinay, M. Sillanpää, A.D. Armour, A. Fefferman, E. Collin, Beyond linear coupling in microwave optomechanics, *Phys. Rev. Res.* **2** (2020) 1306.
- [46] Y.-S. Tang, X.-W. Xu, J.-Q. Liao, H. Jing, L.-M. Kuang, Highly sensitive temperature sensing via quadratic optomechanical coupling

[arXiv:2501.03586](https://arxiv.org/abs/2501.03586), (2025) 1–9.

- [47] A.P. Saiko, V.E. Gusakov, Strongly correlated bistable sublattice and temperature hysteresis of elastic and thermal crystal properties, *JETP* 89 (1999) 92–106.